

Differential dispersal and the Allee effect create power-law behaviour: Distribution of spot infestations during mountain pine beetle outbreaks

James A. Powell¹  | Martha J. Garlick² | Barbara J. Bentz³ | Nicholas Friedenber⁴

¹Departments of Mathematics & Statistics and Biology, Utah State University, Logan, UT, USA

²Department of Mathematics & Computer Science, South Dakota School of Mines and Technology, Rapid City, SD, USA

³USDA-FS Rocky Mountain Research Station, Forestry Sciences Lab, Logan, UT, USA

⁴Applied Biomathematics, Setauket, NY, USA

Correspondence

James A. Powell
Email: jim.powell@usu.edu

Handling Editor: Anna Kuparinen

Abstract

1. Mountain pine beetles (MPB, *Dendroctonus ponderosae* Hopkins) are aggressive insects attacking *Pinus* host trees. Pines use defensive resin to overwhelm attackers, creating an Allee effect requiring beetles to attack en masse to successfully reproduce. MPB kill hosts, leaving observable, dying trees with red needles. Landscape patterns of infestation depend on MPB dispersal, which decreases with host density. Away from contiguously impacted patches (low beetle densities), infestations are characterized by apparently random spots (of 1–10 trees).
2. It remains unclear whether the new spots are spatially random eruptions of a locally endemic population or a mode of MPB spread, with spatial distribution determined by beetle motility and the need to overcome the Allee effect.
3. To discriminate between the hypothesis of population spread versus independent eruption, a model of spot formation by dispersing beetles facing a local Allee effect is derived. The model gives rise to an inverse power distribution of travel times from existing outbreaks. Using landscape-level host density maps in three study areas, an independently calibrated model of landscape resistance depending on host density, and aerial detection surveys, we calculated yearly maps of travel time to previous beetle impact. Isolated beetle spots were sorted by travel time and compared with predictions. Random eruption of locally endemic populations was tested using artificially seeded spots. We also evaluated the relationship between number of new spots and length of the perimeter of previously infested areas.
4. Spot distributions conformed strongly to predicted power-law behaviour. The spatially random eruption hypothesis was found to be highly improbable. Spot numbers grew consistently with perimeter of previously infested area, suggesting that MPB spread long distances from infestation boundaries via spots following an inverse power distribution.
5. The Allee effect in MPB therefore accelerates, rather than limits, invasion rates, contributing to recent widespread landscape-scale mortality in western North America.

KEYWORDS

bark beetle, *Dendroctonus ponderosae*, patchy spread, power-law, travel time

1 | INTRODUCTION

The Allee effect is the accelerating impact of conspecific numbers/densities on some aspect of fitness for small populations (Allee, 1931). At the level of populations, a “demographic” Allee effect is the positive density dependence of population growth rate as population size grows from zero (Stephens, Sutherland, & Freckleton, 1999). Small populations experience Allee effects through several governing interactions that affect individual fitness, including group foraging, defence against predators and mate finding (Lande, 1998). A “strong” Allee effect occurs when growth rates are negative for populations below a critical threshold (Wang & Kot, 2001). Allee effects are common across the animal kingdom and also appear frequently in other organisms (Taylor & Hastings, 2005 and references therein).

Allee effects are often associated with “patchy” spread or invasion (Morozov, Petrovskii, & Li, 2006; Petrovskii, Morozov, & Venturino, 2002). Patchiness can be an emergent, passive response to heterogeneity of space and/or stochasticity of dispersal. For example, genetic diversity of *Spartina alterniflora* clumps in Pacific estuaries improves seed production in plants through hybrid vigour, and consequently occasional accidents of dispersal create diverse clumps with much higher reproduction rates than individuals, creating an Allee effect (Taylor, Davis, Civile, Grevstad, & Hastings, 2004). Patchiness can also develop due to the growth of instabilities and subsequent filtering by the Allee effect (Wang, Shi, & Wei, 2011), a mechanism which also depends on passive dispersal. Gypsy moths (*Lymantria dispar*) spread by stratified dispersal (i.e. short- and long-distance dispersal occur via different processes, with separate dispersal kernels), establishing stable, isolated patches only after episodic long-distance dispersal events that survive the subsequent Allee gauntlet (Sharov & Liebhold, 1998). Environmental heterogeneity can lead to localized populations exceeding the Allee threshold, such as in patches of favourable habitat where the Allee effect is locally reduced. In all of these cases, patchy spread is created by passive dispersal, and the Allee threshold is exceeded indiscriminately, resulting in patch establishment. As more patches are created they coalesce and become a source population (Liebhold & Tobin, 2008).

Species facing strong Allee effects will adapt to overcome them. Allee (1931) himself recognized that aggregation was the primary mechanism by which species increase survival rates and argued that only in the simplest organisms would aggregation be happenstance. Except in rare, small, well-mixed systems, populations are likely to have active dispersal adaptations for aggregating individuals. Understanding the population-level expression of the Allee effect will require understanding the aggregation mechanisms. Example mechanisms include habitat selection in heterogeneous environments (Greene, 2003), congregation via density-dependent dispersal (Turchin, 1989) and pheromone responses in arthropods (Wertheim, van Baalen, Dicke, & Vet, 2005). Aggregations that result from active dispersal at low population densities will draw down surrounding populations and lead to spatial trade-offs which

may be expressed independently from those occurring as a result of landscape heterogeneity. Moreover, when the landscape offers varying resistance to movement, aggregation should be more likely in patches that are easier to access or cause bottlenecks to otherwise fluid movement. Thus, patterns of patchy spread in species actively aggregating to overcome Allee effects could be markedly different than in species with indiscriminate patch creation.

The mountain pine beetle (MPB, *Dendroctonus ponderosae* Hopkins) provides an excellent opportunity to study active patch formation in a species facing an Allee effect. MPB is an economically and ecologically important native species that has caused significant mortality in *Pinus* forests across the western United States and Canada (Meddens, Hicke, & Ferguson, 2012). Due to its economic impact, there is an impressive amount of scientific information on MPB, and it has been established that active dispersal processes at large and small spatial scales play a central role in population outbreak dynamics (Logan, White, Bentz, & Powell, 1998; Powell & Bentz, 2014).

Unlike many phytophagous insects, successful MPB reproduction usually results in death of all or part of the host. Host trees have evolved varying chemical and resin responses that reduce vulnerability to attack by bark beetles and their fungal and bacterial associates (Boone et al., 2013; Kane & Kolb, 2010; Raffa, Powell, & Townsend, 2012). Vigorous, well-defended trees require rapid attack and colonization by a large number of beetles (i.e. a mass attack) to outpace tree responses (Berryman, Dennis, Raffa, & Stenseth, 1985), leading to a strong Allee effect for the beetles. Conversely, trees stressed by biotic and abiotic agents have a reduced capacity for defence and can be overcome by low numbers of beetles (Raffa, Aukema, Erbilgin, Klepzig, & Wallin, 2005; Safranyik & Carroll, 2006). The better defended, more vigorous trees tend to be larger and have higher nutritional quality thereby leading to a positive feedback as beetle population density increases (Boone, Aukema, Bohlmann, Carroll, & Raffa, 2011; Raffa et al., 2008).

Epidemic MPB population dynamics are well-described by phenology, host-dependent dispersal and the Allee effect (Powell & Bentz, 2009, 2014). Beetles emerge daily from previously infested hosts and disperse with motility decreasing exponentially with host density. Where the dispersed population exceeds the Allee threshold new hosts are successfully colonized. Powell and Bentz (2014) showed that this combination of mechanisms describes 85% of the observed spatial pattern of beetle-killed trees on kilometre scales. Interestingly, where the Powell and Bentz (2014) model missed predicting observed impacts (approximately 8% of the landscape), the type of impact was small, isolated spots. These spots represent a trivial portion of a given year's MPB footprint during an epidemic, but the evolving pattern in subsequent years depends strongly on the density and spatial location of spots across the landscape.

Regardless of whether satellite spots are caused by beetles dispersing from the main body of an outbreak, spot initiation and growth depends on MPB movement, conditioned by host tree availability and size, MPB population size, weather and behaviour-modifying chemicals (Mitchell & Preisler, 1991; Safranyik, Linton,

Silversides, & McMullen, 1992). Host kairomones play a significant role by signalling trees that are under stress caused by biotic and abiotic factors (Chapman, Veblen, & Schoennagel, 2012; Goheen & Hansen, 1993). At lower beetle densities, after a weakened tree is found, aggregation is facilitated by pheromones, which through a synergistic reaction with host defensive compounds attract additional beetles (Raffa et al., 2005), resulting in mass attacks on a single tree. Following aggregation to one or several weakened trees, the number of adult beetles necessary to overcome the Allee effect on more vigorously defended host trees become available and attacking beetles switch to nearby trees, creating a spot with one to several killed hosts. We hypothesize that spot creation is not indiscriminate, but instead that the spatial distribution of MPB spots are the result of dispersers leaving the perimeter of previously affected areas, spreading differentially due to host-dependent motility and aggregating locally to mass attack trees. Furthermore, we suggest that the spatial distribution of spots reflects landscape resistance to beetle movement.

MPB are not likely to disperse to distant focus trees if acceptable hosts are encountered first. Powell and Bentz (2014) calibrated a model of MPB movement based on host tree density-derived beetle motility wherein resistance to beetle movement increases exponentially with host tree density. Assuming that potential spot foci are randomly distributed per capita among hosts, we argue that the distribution of spots should follow a power-law distribution in travel time along landscape paths of least resistance from beetle sources. The power law, in which spatial probability of spot occurrence is proportional to a negative power of travel time, arises because increasing encounter rates for weakened focal trees correlate with decreasing motility as host densities increase. Moreover, because the perimeter of previously infested areas would be the primary source of dispersers, we hypothesize that the yearly number of new spots should scale with perimeter size.

We test these hypotheses using aerial surveys of MPB-caused tree mortality and host tree density data for three study areas in Idaho, Washington and Colorado. Annual occurrence of isolated spots were identified and travel time between each spot and the nearest contiguous area of MPB-killed trees that could provide a beetle source was recorded. The distribution of observed spots in travel time was determined, and the number of spots compared with the perimeter size of previously infested areas. An alternate hypothesis, that spots occur as random eruptions of an endemic beetle population, was also examined. The observed number of spots each year were seeded spatially at random and tested for possible power-law behaviour. We found that the power-law hypothesis was strongly supported across many years of observations, while random eruption was highly improbable. Yearly spot numbers scale with a rough measure of the size of the perimeter of previous infested areas, supporting the contention that beetles disperse from the edges of major infestations to invade new areas via spots. Accelerating invasion rates are one consequence of power-law dispersal, which is consistent with observations of MPB's explosive spread in western North America.

2 | MATERIALS AND METHODS

2.1 | Study areas

2.1.1 | Sawtooth study area

The Sawtooth study area in central Idaho (Figure 1) is a rectangular region from approximately 44°22'N to 43°44'N (~60 km) and 115°10'W to 114°28'W (~30 km), comprising over 180,000 ha, including the Sawtooth National Recreation Area. A single host, lodgepole pine, predominates from 1,650 to 2,000 m and grows in stands with relatively homogeneous demographics at the lowest elevations. The landscape is characterized by a valley and surrounding mountains, with elevations from 1,650 to 3,600 m. Vegetation types range from shrub and grasslands to coniferous forests with lodgepole pine, Douglas fir (*Pseudotsuga menziesii* (Mirb.) Franco), subalpine fir (*Abies lasiocarpa* [Hook.] Nutt), and whitebark pine (*P. albicaulis* Engelm.) at higher altitudes. Densities of pine average 450 trees/ha, although the valley includes many dense stands of 1,000 trees/ha as well as meadows and pasture land with no hosts. Extensive barren areas exist above tree-line at the highest elevations. Between 1995 and 2005, a MPB outbreak occurred throughout the Sawtooth study area, impacting more than a third of the pine host type (Pfeifer, Hicke, & Meddens, 2011).

2.1.2 | Chelan study area

The Chelan study area in northern Washington (Figure 1) encompasses 446,000 ha, from approximately 47°56'N to 48°35'N and from 119°

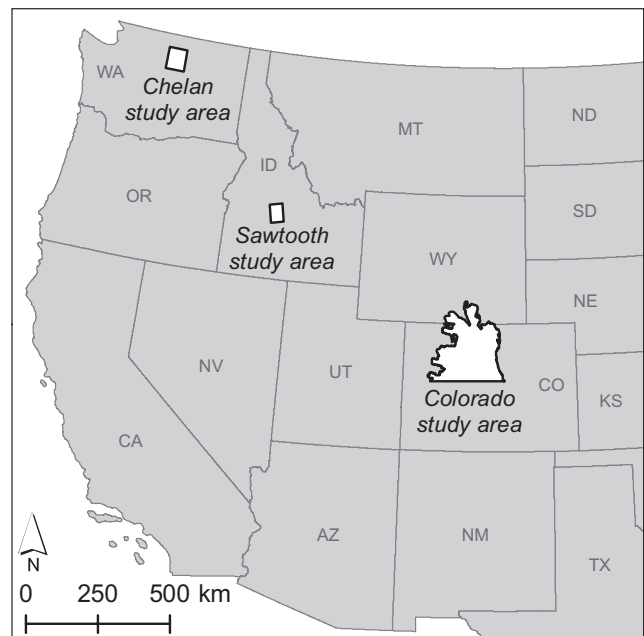


FIGURE 1 Study areas used in this paper. All study areas had at least 10 years of continuous aerial detection survey for mountain pine beetle impact. An outbreak occurred between 1995 and 2005 in the Sawtooth and between 2001 and 2010 in Colorado. In the Chelan study area, multi-modal impact occurred over 20 years, peaking in 2008

52°W to 120°44'W. Elevations range from 336 m at Lake Chelan to peaks at 2,700 m. The study area is comprised of public and private lands, including portions of the Methow Valley and Chelan Ranger Districts, Okanagan-Wenatchee National Forest and North Cascades National Park. The Methow River drainage characterizes the eastern half of the study area. Coniferous vegetation within the study area include ponderosa pine (*P. ponderosa*), lodgepole pine, whitebark pine, Englemann spruce (*Picea engelmannii* Parry) and Douglas fir, with host pine trees averaging 500 trees/ha. The Chelan study area boundary was chosen to encompass pine vegetation susceptible to MPB infestation and active MPB patches based on ground surveys. MPB impact began in the late 1990s and peaked in 2008 (Crabb, Powell, & Bentz, 2012).

2.1.3 | Colorado study area

The Colorado study area contains over 4,380,000 ha in northern Colorado, including Rocky Mountain National Park, North Park and several of Colorado's highest peaks (Figure 1). Elevations range from 1,700 m on the Front Range west of Fort Collins to over 4,300 m at Longs Peak. The study area begins roughly at Interstate 70 in the south and reaches in the north to approximately 41°50'N (into southern Wyoming), in the east to 105°0'W, and in the west to 108°0'W, encompassing portions of the Medicine Bow-Routt and Arapaho-Roosevelt National Forests. The southern boundary along the route of I-70 was chosen as a natural break in MPB impacts, and western boundaries were chosen to encompass impacted regions as far to the west as Glenwood Springs. Conifers include lodgepole and limber pines (*P. flexilis*), Englemann spruce, subalpine fir and Douglas fir, and average pine host densities are 780 trees/ha across the area. Significant MPB impact began in the early 2000s and peaked in 2007 (Crabb et al., 2012).

2.2 | Data sources

2.2.1 | Pine density data

Spatially explicit datasets of pine density at 30-m resolution were derived for the study areas using existing geospatial datasets of vegetation composition and structure. Briefly, for the Sawtooth and Colorado study areas forest density (trees per hectare >2.54 cm DBH) at 250-m resolution, developed by the USDA Forest Service FIA (Blackard et al., 2008), were downscaled to 30-m resolution using data from the inter-agency Landscape Fire and Resource Management Planning Tools Project (LANDFIRE). Data from the GNNFire project (LEMMA, 2005; Pierce, Ohmann, Wimberly, Gregory, & Fried, 2009) were used to derive pine density matrices of potential pine hosts for the Chelan study area at 30-m resolutions. Methods for all study areas are described in detail by Crabb et al. (2012).

2.2.2 | Aerial detection survey data

Geo-referenced data describing the annual number of MPB-killed trees were obtained for all three study areas beginning in 1991 for the Sawtooth, 1980 for Chelan and 2001 for northern Colorado (USDA

Forest Service, <http://www.foresthealth.info/portal>). The aerial detection surveys (ADS) are conducted in fixed-wing aircraft by trained observers who manually record numbers of killed trees based on the colour of tree foliage (Halsey, 1998). Foliage of dead, beetle-killed trees changes from green to red within a single year, and in subsequent years the foliage turns grey and needles are lost. ADS datasets include polygon shapefiles with metadata describing the estimated number of trees per acre affected and a code for the damage causal agent(s). Polygons depicting MPB impact were queried using their unique code. Rasters of total MPB impact by year were created by summing MPB impacts across all pine host types for each polygon then converting to 30-m rasters. For purposes of this study, rasters were converted to either one or zero to indicate whether or not MPB infestation was observed in a pixel on a given year. Rasters were kept in the coordinate system of the ADS shapefiles, North American Datum 1983 Albers, and other geospatial raster data used in this study were converted to this projection at 30-m resolution using ArcGIS 9.3 software (ESRI, 2008).

2.2.3 | Diagnosing isolated spots

We defined a spot as a single 30-m pixel with MPB impact, surrounded by pixels with no impact. Let ADS_{ij}^n indicate the presence (1) or absence (0) of MPB impact in a pixel in row i , column j of the ADS raster for year n . To determine the location of a potential isolated spot, we applied a discrete second derivative test, recording all positions below 50% of the maximum second derivative for the year,

$$\Delta ADS_{ij}^n \stackrel{\text{def}}{=} \frac{1}{\Delta x^2} \left(ADS_{i+1,j}^n + ADS_{i-1,j}^n + ADS_{i,j+1}^n + ADS_{i,j-1}^n - 4ADS_{ij}^n \right) \leq -\frac{1}{2} \max_{ij} \left| \Delta ADS_{ij}^n \right|,$$

where Δx is the pixel width (30 m). The minus sign is used because spots are local maxima with large negative concavity. Each potential spot was then screened to test whether the eight surrounding pixels were impact-free (guaranteeing it to be separated from contiguous regions of impact). The list of verified spot locations in a year were recorded for further analysis.

2.3 | Determining travel times to spots from previously infested areas

2.3.1 | Resistance to movement, motility and pixel residence time

The ecological diffusion model (Turchin, 1998) describes the population-level distribution, $P(x,y,t)$, that emerges from individual random walks with movement probabilities based on local habitat information:

$$\frac{\partial P}{\partial t} = \left(\frac{\partial^2}{\partial x^2} + \frac{\partial^2}{\partial y^2} \right) [\mu(x, y)P]$$

(Okubo & Levin, 2001; Patlak, 1953). The individual movement probability at any point in space is proportional to the "motility" at that point, $\mu(x,y)$, resulting in variable patch residence times which are inversely proportional to μ . In a homogeneous environment, motility

is the same as the diffusion constant and has units of area per time. In variable environments, ecological diffusion is very different from standard ("Fickian") diffusion, in which the diffusion constant is intermingled with derivatives (e.g. $\frac{\partial}{\partial x}(D(x)\frac{\partial p}{\partial x})$ in one dimension). In ecological diffusion, all spatial derivatives apply to the product of motility and population density ($\mu(x, y)P$), supporting "weak" solutions with discontinuities where habitat types change and long-term solutions with densities inversely proportional to motility leading to aggregation in favourable (high residence time) habitat. Intuitively, the mathematical justification for ecological diffusion is that the diffusion process applies only to those individuals choosing to leave a patch (the number of which is proportional to μP , the product of movement probability and the density available to depart). Thus, the Laplacian, $\frac{\partial^2}{\partial x^2} + \frac{\partial^2}{\partial y^2}$, applies only to the moving population, μP . More mathematical details about the differences between ecological and Fickian diffusion, and the consequences for large-scale population movement, can be found in Garlick, Powell, Hooten, and McFarlane (2011).

Motility in a patch is inversely related to mean residence times for individuals in the patch (Turchin, 1998); in a pixel with area Δx^2 the expected residence time of individuals is

$$\Delta T = \frac{\Delta x^2}{\mu}.$$

For MPB, Powell and Bentz (2014) showed that beetle populations have motility following a negative exponential with host density,

$$\mu = \mu_0 \exp \left[-(\mu_1 + \ln(\mu_0)) \frac{S_{ij}}{1,000} \right] = \mu_0 \exp [-\hat{\mu}_1 S_{ij}], \quad (1)$$

where S_{ij} is the density of hosts in pixel ij , scaled in thousands of hosts per hectare, μ_0 is the maximum motility (3.79 km²/day) in the absence of hosts, and $\mu_1 = -10.9$ is the relative rate of motility decline with host density. This model for motility reflects the time spent by beetles searching an increasingly complex environment for chemical plumes and potentially susceptible hosts. The parameter $\hat{\mu}_1 = \frac{\mu_1 + \ln(\mu_0)}{1000} = 1.3472 \times 10^{-3}$ is introduced for convenience. Converting to minutes during a 10-hr flight day, this model gives a mean residence time of 64 min in a 30-m pixel containing a density of 500 hosts/ha. Residence time in a pixel with no trees is 8.5 s (corresponding to an average speed of 3.5 m/s for MPB crossing unforested pixels). This variability in residence times causes beetles to disperse rapidly through areas with few hosts and aggregate in areas with higher host density.

2.3.2 | Minimum travel time for attacking MPB

If a beetle follows a path passing through K pixels, $\{(i_k, j_k)\}_{k=1}^K$, the expected travel time is

$$\sum_{k=1}^K \frac{\Delta x^2}{\mu_0} e^{\hat{\mu}_1 S_{i_k, j_k}}. \quad (2)$$

Paths followed by beetles when participating in a spot attack cannot be known a priori. However, beetles are more likely to be successful at overcoming host defences in locations where travel times to beetle

sources are shorter. We therefore hypothesize that observed spots will be structured according to *minimal* travel times from the nearest beetle sources.

The minimum travel time to a point in a landscape, T , satisfies the eikonal equation,

$$\|\nabla T\| = \sqrt{T_x^2 + T_y^2} = \frac{\Delta x}{\mu_0} e^{\hat{\mu}_1 S}, \quad (3)$$

which connects minimum travel times (T) and residence times through the gradient vector, $(T_x, T_y) = \nabla T$ (subscripts indicate partial derivatives). In Equation (1), the temporal cost of movement from one pixel to the next (i.e. the rate of change of travel time) is proportional to how long beetles spend in the space between (i.e. the residence time). The eikonal equation is difficult to solve analytically, but can be efficiently solved numerically using the fast sweeping method (Zhao, 2004). This approach iterates to a solution in a pixel by examining neighbours to determine which has the lowest travel time, then updating projected travel time by adding the current pixel's residence time to the minimum among nearest neighbours.

Because beetles come from trees infested in the previous year we use ADS data in year $n - 1$ to set $T_{ij} = 0$ in pixels with source populations of beetles. The fast sweeping method then generates minimal travel times from the perimeter of observed ADS impact in the previous year to all other points on the landscape, conditioned by intervening host density which alters motility in pixels between spots and the nearest sources (1). In every year, the travel time map is different because the location of source populations changes. Figure 2 depicts projected travel times for a portion of the Sawtooth study area for 2001.

Observed travel times at spot locations were recorded yearly, using that year's spatial pattern of travel times resulting from host densities and ADS impact from the previous year. Across all years in each study area (8 in the Sawtooth, 10 in Colorado and 20 in Chelan), a histogram of observed travel time to spots was created. The number of bins was chosen so that the bin corresponding to the largest travel times held at least one percent of the total number of observations. The bin containing zero travel time was ignored (as a peculiarity of the ADS data is that isolated spots are sometimes observed inside polygons indicating contiguous impact in the previous year, see Figure 2 for an example). In each case, a power-law curve was fit to the binned observations using nonlinear maximum likelihood on the arithmetic scale and assuming normal distribution of errors.

2.4 | Predicted distribution of spots

We assume that spots where beetles have overcome the Allee effect are most likely at foci located with minimal travel time from source populations. Consider a beetle path passing through K pixels, $\{(i_k, j_k)\}_{k=1}^K$. If potential foci are randomly distributed among hosts, the probability of passing through pixel k and *not* encountering a weakened focus tree is $\exp[-\alpha \Delta x^2 S_{i_k, j_k}]$, where α is the per capita encounter rate for weakened trees. The probability of passing pixel K on the path is therefore

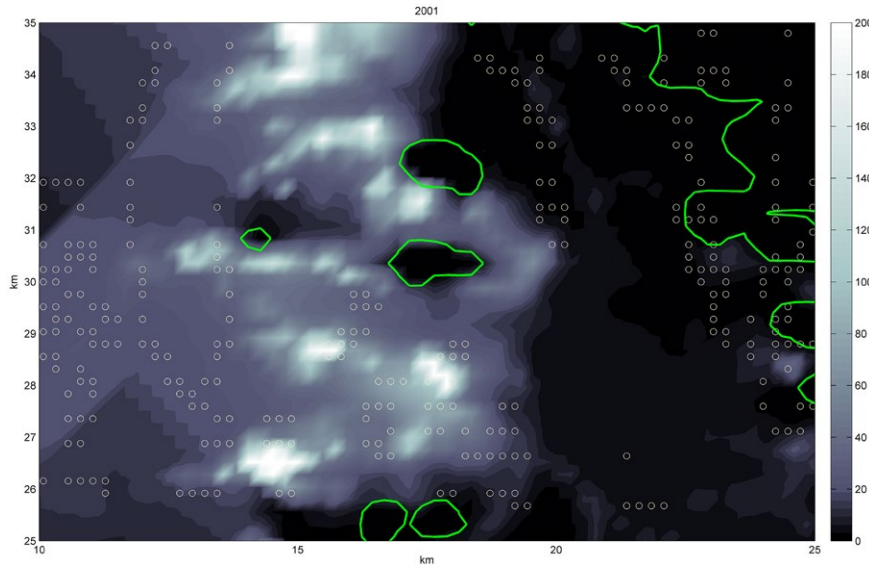


FIGURE 2 Travel time (in minutes, see colour bar to right) from beetle sources (boundaries indicated by solid contours) to other locations in a 10 × 15 km portion of the Sawtooth study area, 2001. New spots identified in the annual ADS appear as circles. Occasionally spots are observed in previously impacted area, as indicated by circles inside of solid contours

$$P(k > K) = \prod_{k=1}^K e^{-\alpha \Delta x^2 S_{k,j_k}}$$

Minimizing travel time to the final pixel requires that the path encounter as few hosts as possible to reduce time in intervening pixels, so $S_{k,j_k} \ll S_{k',j_{k'}}$ on paths that end in isolated spots. The probability of passing pixel K becomes

$$P(k > K) = \prod_{k=1}^K e^{-\alpha \Delta x^2 S_{k,j_k}} \approx e^{-\alpha \Delta x^2 S_{K,j_K}} \quad (4)$$

because $\exp(-\alpha \Delta x^2 S_{k,j_k}) \approx 1$ for the earlier, low-density pixels along the path. Actual travel time along the path will be dominated by the contribution of the final, most densely stocked pixel, giving an approximate travel time to pixel K of

$$T_K \approx \frac{\Delta x^2}{\mu_0} e^{\beta_1 S_{K,j_K}} \quad (5)$$

We can now find the cumulative density function (CDF) for $T \leq T_K$, using (4),

$$P(T \leq T_K) = 1 - P(k > K) \approx 1 - e^{-\alpha \Delta x^2 S_{K,j_K}} \quad (6)$$

Equation (5) can be rearranged to express density in the final pixel as a function of T_K ,

$$e^{S_{K,j_K}} \approx \left[\frac{\mu_0}{\Delta x^2} T_K \right]^{\frac{1}{\beta_1}}$$

and now the CDF, (6), can be written in terms of T_K alone,

$$P(T \leq T_K) \approx 1 - \left[\frac{\mu_0}{\Delta x^2} T_K \right]^{-\frac{\alpha \Delta x^2}{\beta_1}} \quad (7)$$

The probability density function, $p(T)$, for travel times to spots is proportional to the derivative of (7),

$$p(T) \propto T^{-\left(1 + \frac{\alpha \Delta x^2}{\beta_1}\right)}, \quad (8)$$

giving a power law in minimal travel time.

2.5 | Relating spot numbers and perimeter of previously impacted areas

If active spot formation is a mode of dispersal that allows MPB to invade new areas, one would expect the number of new spots formed each year to scale roughly with the perimeter of the infested area in the previous year, as the perimeter is the primary source of dispersers. However, the shapes of contiguously impacted regions are spatially complex, making direct measurement of the total perimeter length untenable. Instead, we adopt the approach of Shigesada and Kawasaki (1997), who used square root of impacted area as a surrogate for perimeter. In each year, the total impacted area was calculated by summing all pixels with ADS impact and subtracting the number of new spots for that year (as each spot has been filtered to impact only a single pixel). The number of spots in year n was then fit to the square root of impacted area in year $n - 1$ using linear regression.

2.6 | An alternative: Random spot formation

To test an alternative hypothesis that spots form randomly in space, we generated artificial datasets of isolated spots. For each year and in each study area, random indices were chosen from discrete uniform distributions with the only restriction being that a “spot” location must appear in an area with host cover type. Random locations were generated until the number of “spots” was equal to the number of observed spots in that year for that study area. The random spot distribution was fit to a power-law using nonlinear regression, and the predicted cumulative distribution calculated directly by analytic integration from the smallest travel time:

$$F(T) = \hat{\alpha} T_{\min} \int_{T_{\min}}^T t^{-(1+\hat{\alpha})} dt = 1 - \frac{T_{\min}^{\hat{\alpha}}}{T^{\hat{\alpha}}},$$

where $1 + \hat{\alpha}$ is the (negative) fitted exponent and the coefficient in front of the integral normalizes the distribution. To test the

hypothesis that the data were actually generated by a power-law distribution “spots” were binned according to travel time from previous year’s impacted area and goodness of fit tested using Cramér-von Mises’ A^2 (as recommended by Choulakian, Lockhart, & Stephens, 1994). The statistic tests the correspondence between observed and predicted cumulative distributions, and is defined for discrete observations:

$$A^2 = \frac{1}{N} \sum_{j=1}^{k-1} \frac{Z_j^2 p_j}{H_j(1-H_j)},$$

where N is the number of spots, k is the number of bins, and if e_j and o_j are the number of expected and observed spots in bin j , then $p_j = \frac{e_j}{N}$ and

$$S_j = \sum_{i=1}^j o_i, \quad T_j = \sum_{i=1}^j e_i, \quad Z_j = S_j - T_j, \quad \text{and} \quad H_j = \frac{1}{N} T_j$$

(Choulakian et al., 1994). Calculated A^2 were compared with tabulated critical values, A_{crit}^2 , using degrees of freedom corresponding to the number of bins (k) + number fitted parameters (2) – 1 to determine whether the null hypothesis (random spots follow a power-law distribution) can be rejected with 90% confidence.

3 | RESULTS

3.1 | Spot distributions and relation to perimeter size of previous year infestations

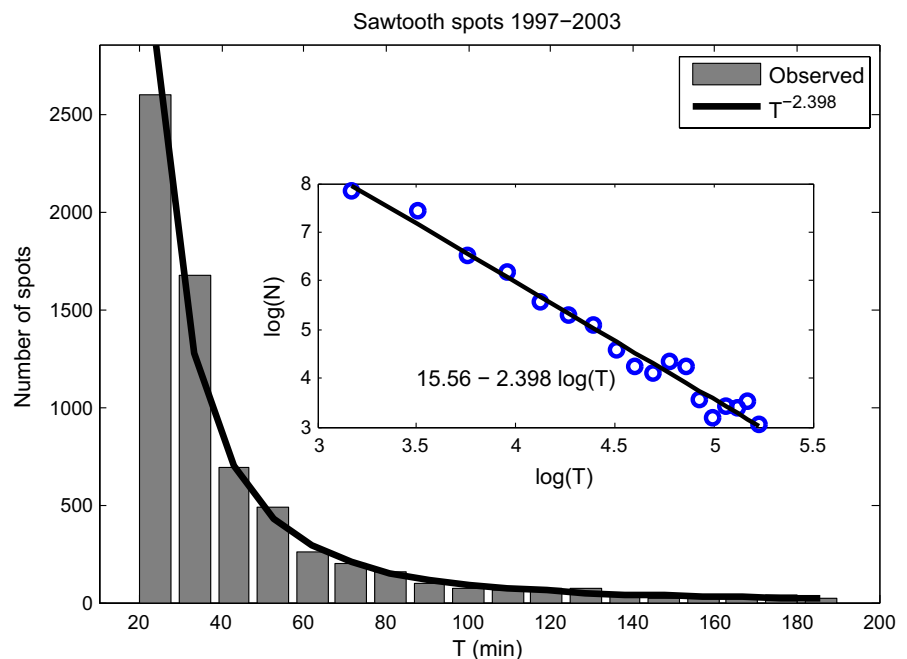
In the Sawtooth study area, nonlinear regression gave an exponent of -2.398 and $r^2 = .990$ (Figure 3). The predicted exponent is $1 + \frac{\alpha\Delta x^2}{\beta_1}$, indicating $\alpha\Delta x^2 = 0.0102$, or 10.2 potential focus trees per

1,000 trees. In Chelan, the predicted exponent was lower, -1.215 , fitted with $r^2 = .998$ (Figure 4). This lower exponent indicates that the per-capita rate of focus tree encounter was $\alpha\Delta x^2 = 0.00158$, or 1.58 focus trees per 1,000 trees. Results from Colorado were close to the Chelan results, with $\alpha\Delta x^2 = 0.00201$ and $r^2 = .985$ (Figure 5). Viewed in terms of focus trees per hectare, using average host densities to convert encounter rates to potential focus tree densities, rates varied from 0.79 trees/ha in Chelan to 1.56 trees/ha in Colorado and up to 4.59 trees/ha in the Sawtooth study area. These spot initiation rates compare favourably with the observations of Carroll et al. (2006) in British Columbia. On seven study plots, these authors observed isolated mass attacks of MPB corresponding to incipient epidemics in 2000–2004 and reported spot densities varying from a low of .403 trees/ha to a high of 4.04 trees/ha with a mean of 1.78 trees/ha.

The number of spots formed in a year is expected to increase with the perimeter of area impacted in the previous year, and perimeter scales with the square root of impacted area, provided the shape of the impacted areas is not too complex. Following Shigesada and Kawasaki (1997), we fit the number of spots observed in year n , N_n , to the square root of the previous year’s impacted area, $A_{n-1} = \sum_{i,j} ADS_{ij}^{n-1}$, using simple regression. Regression coefficients were consistent, although goodness of fit varied:

Study area	Fitted model	Coeff. determination	Graph
Sawtooth	$N_n = 82.7\sqrt{A_{n-1}}$	$r^2 = .939$	Figure 6
Chelan	$N_n = 78.9\sqrt{A_{n-1}}$	$r^2 = .327$	Figure 7
Colorado	$N_n = 75.9\sqrt{A_{n-1}}$	$r^2 = .784$	Figure 8

FIGURE 3 Distribution of predicted travel times (minutes) to observed spots in the Sawtooth study area between 1997 and 2003. Travel times to observed spots were placed in 20 bins; the bin containing zero was not included. Best maximum likelihood fit of a power law to the histogram is depicted in as a solid line; linearity of the data and the fitted curve are depicted on log–log scale in the inset. The fitted curve describes 99.0% of the variability in the data according to r^2



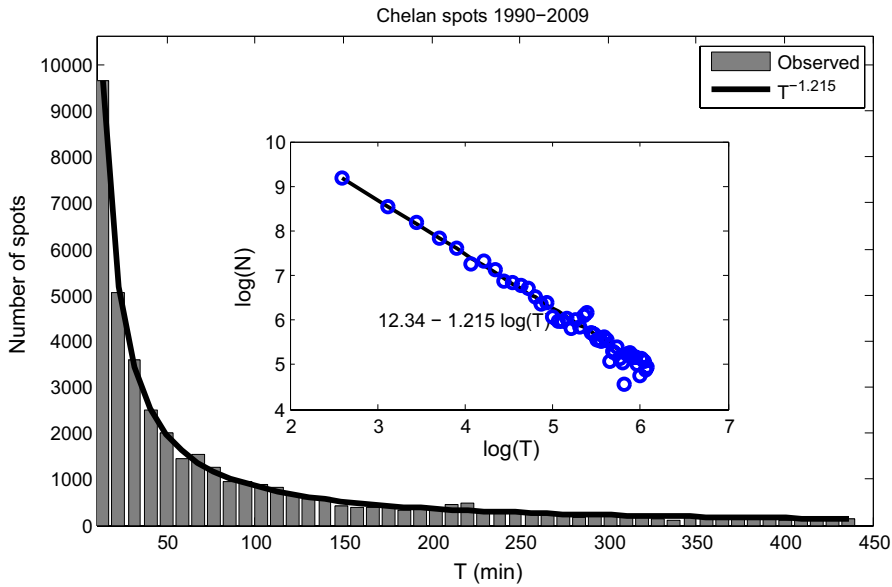


FIGURE 4 Distribution of predicted travel times (minutes) to observed spots in the Chelan study area between 1990 and 2009. Travel times to observed spots were placed in 22 bins; the bin containing zero was not included. Best maximum likelihood fit of a power law to the histogram is depicted as a solid line; linearity of the data and the fitted curve are depicted on log–log scale in the inset. The fitted curve describes 99.8% of the variability in the data according to r^2

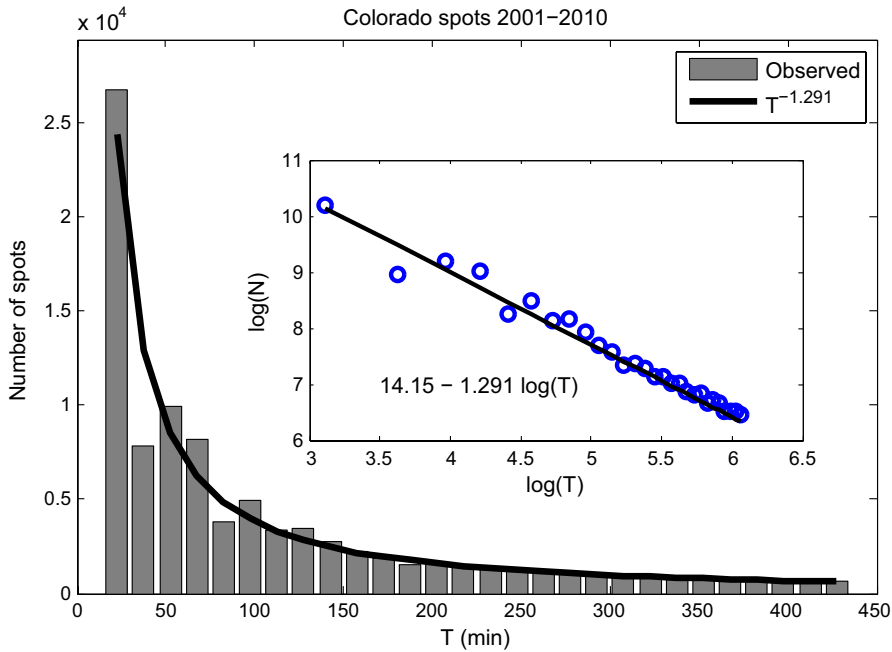


FIGURE 5 Distribution of predicted travel times (minutes) to observed spots in the Colorado study area between 2002 and 2010. Travel times to observed spots were placed in 25 bins; the bin containing zero was not included. Best maximum likelihood fit of a power law to the histogram is depicted as a solid line; linearity of the data and the fitted curve are depicted on log–log scale in the inset. The fitted curve describes 98.5% of the variability in the data according to r^2

The fitted curves are displayed in terms of impacted area and year of impact in Figures 6–8. As expected, the number of spots increases with the size of the main infestation and in particular with a rough measure of infestation perimeter, with between 75 and 83 spots generated per kilometre of perimeter. This supports the idea that beetles creating isolated spots travel from the perimeter of major infestations in the surrounding landscape.

3.2 | Random seeding of spots

To illustrate the differences between random formation of spots and the power-law distribution of spots, we seeded forested areas with artificial “spots” whose locations were selected from a uniform

distribution over areas with host cover type. In each study area, in each year as many random “spots” were generated as were actually observed in that year, and the spot numbers binned according to the year’s travel time map in the same way as the observed spots (Figure 9). The Cramér–von Mises A^2 statistic was calculated for each study area.

Study area	A^2	df	A^2_{crit}	Result
Sawtooth	63.95	20	1.834	Reject ($p < .0001$)
Chelan	1.842	22	1.835	Reject? ($p < .1$)
Colorado	73.12	25	1.837	Reject ($p < .0001$)

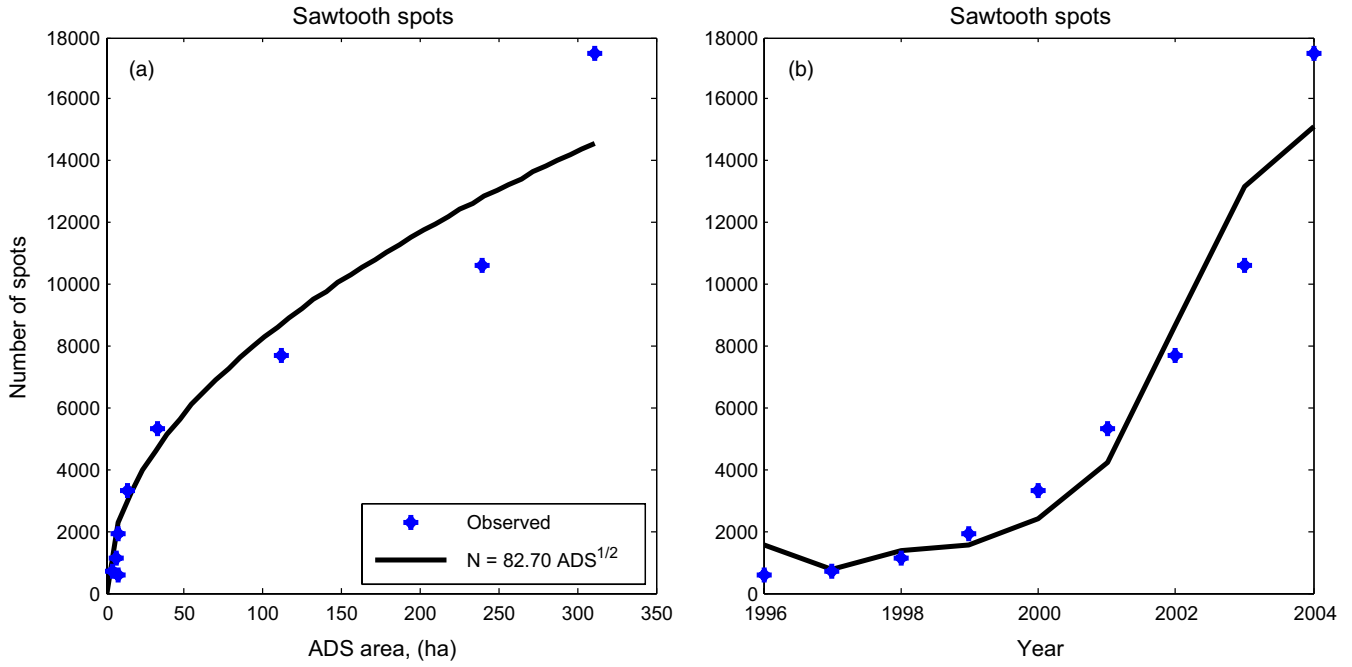


FIGURE 6 Observed spots in the Sawtooth study area between 1996 and 2004 as a function of infested area perimeter. In (a) observed spots (*) are fitted to $\sqrt{\text{Impacted Area}}$; fit has $r^2 = .939$. In (b) both number of observed spots (*) and predicted number of spots (solid line) are plotted as a function of year. The quality of the fit indicates that the number of spots is predicted by the perimeter of the infested area, as would be expected if beetles from the edge of the infested area overcome the Allee effect by active dispersal to spots

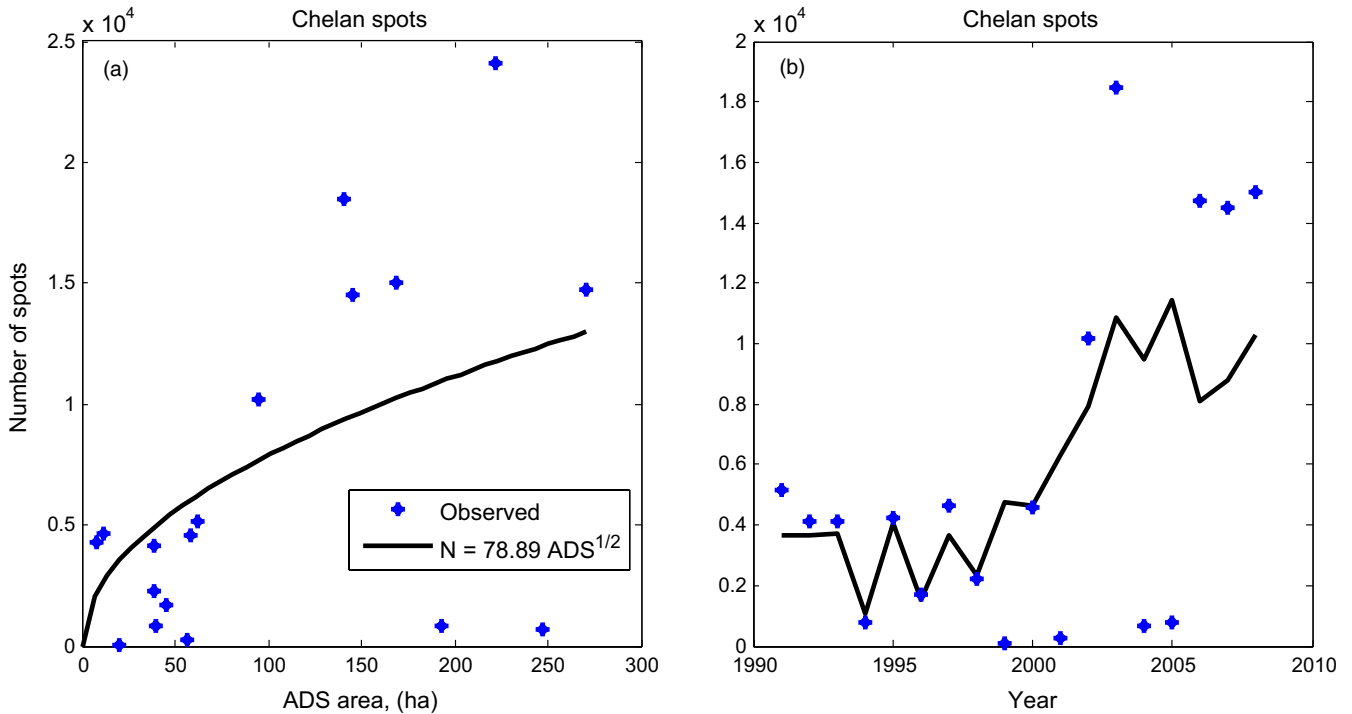


FIGURE 7 Observed spots in the Chelan study area between 1990 and 2010 as a function of infested area perimeter. In (a) observed spots (*) are fitted to $\sqrt{\text{Impacted Area}}$; fit has $r^2 = .327$. In (b) both number of observed spots (*) and predicted number of spots (solid line) are plotted as a function of year. The Chelan series of infestations occurred in several geographically separated areas, and the years with very low spot formation correspond to the collapse of a sub-infestation because available hosts were exhausted

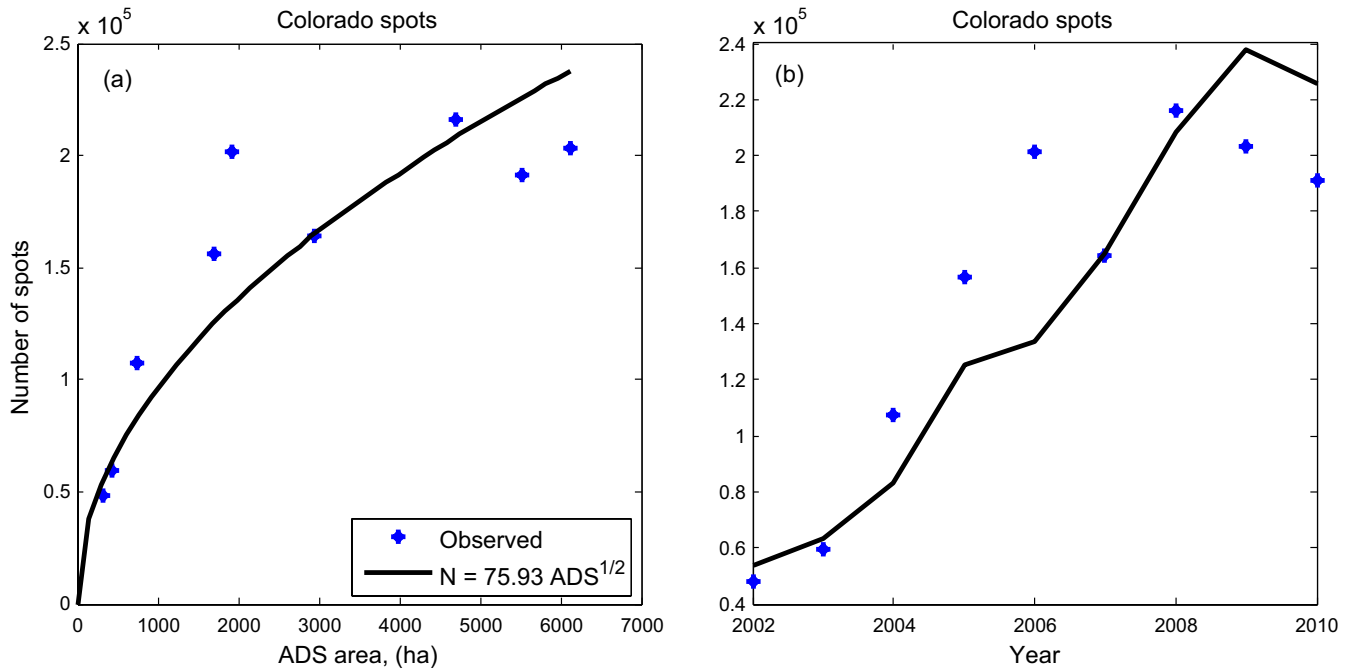


FIGURE 8 Observed spots in the Colorado study area between 2002 and 2010 as a function of infested area perimeter. In (a) observed spots (*) are fitted to $\sqrt{\text{Impacted Area}}$; fit has $r^2 = .784$. In (b) both number of observed spots (*) and predicted number of spots (solid line) are plotted as a function of year. The Colorado outbreak spread through a much larger area, but number of spots correlates strongly with perimeter, indicating that beetles from the edges are overcoming Allee effects by active dispersal to spots

In the cases of the Sawtooth and Colorado study areas, the hypothesis that the randomly generated “spots” followed a power-law distribution in travel time from previously impacted areas could be rejected with a high degree of confidence. In the Chelan study area, the pattern of spots was more random. While it is not clear why the Chelan data did not more closely adhere to the power-law prediction, we note that the area had substantially lower spot densities and stronger spatial structure to its host population.

4 | DISCUSSION

We have shown that a strong Allee effect, requiring beetle aggregation to overcome host pine defences, in combination with landscape resistance, in which motility decreases exponentially with host density, leads to dispersive spread via spots under a power-law distribution of travel times from source populations. Low densities of beetles, dispersing from the perimeter of previous infested areas, aggregate at weakened focus trees which nucleate isolated spots. The impact of the Allee effect is that aggregation away from major infestations draws down the dispersing beetle population so that more spots are possible at locations with lower travel time, with algebraically fewer spots in regions with higher travel time. Aerial surveys of annual MPB infestation in Idaho, Washington and Colorado study areas were analysed and found to conform very strongly to the power-law prediction ($r^2 \geq .985$). The alternate hypothesis that spots arise spontaneously,

was not supported in Idaho and Colorado, however, spontaneous spot creation could not be ruled out in the Washington (Chelan) study area.

Our results also suggest that dispersing beetles leave the perimeter of source infestations (as measured by square root of impacted area), although this was less strongly supported ($.327 \leq r^2 \leq .939$). A low correlation was potentially due to the poor relationship between the actual and estimated (square root of impacted area) perimeter size, in addition to the fact that we did not account for temperature-dependent differential MPB productivity among years, which is known to have a substantial impact on population growth (Powell & Bentz, 2009). Nevertheless, the number of spots created had a consistent relationship to previous year infestation perimeter, and the relationship was strongest in the smallest (Sawtooth) study area, where the spatial structure of MPB-caused tree mortality was geographically simplest. In Colorado, the largest study area, hosts had a relatively homogeneous distribution but mountainous topography broke up large areas of infestation, weakening the relationship between perimeter and spot numbers. In the Chelan area, where the relationship was only marginally significant, the MPB outbreak was dissected into three areas separated by deep river valleys, causing asynchronous and separated MPB activity. Clear outliers with low numbers of spots occurred in years when the intensity of MPB activity shifted between the areas. Large bodies of water, deep valleys with no hosts and high-altitude ridges may have obscured the power-law process of spot formation through disruption of dispersal and strong spatial structuring of potential hosts.

In heterogeneous environments, the power-law theory predicts that MPB spread preferentially along corridors of relatively high

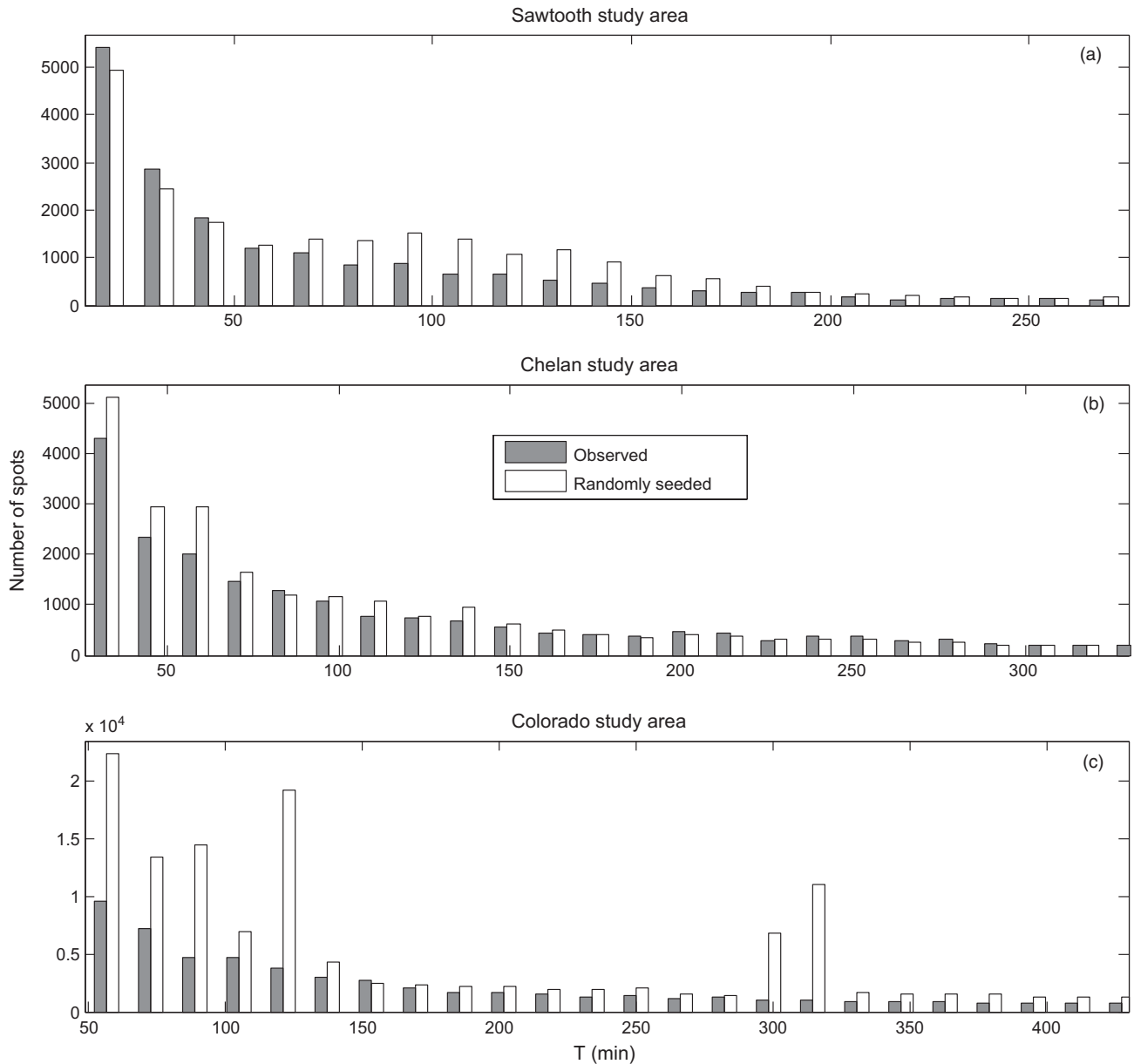


FIGURE 9 Comparison of travel time histograms for observed (solid bars) and randomly seeded (open bars) spots in the three study areas. The same number of random spots were generated yearly as were observed, with random spots sampled from a uniform distribution in locations with host cover type. In the Sawtooth (a) and Colorado (c) study areas, the distributions of randomly select spots are multi-modal and clearly not of power-law type. In Chelan (b) the distribution is unimodal, and could not be rejected as a potential power-law distribution. Spot densities were substantially lower in Chelan and many barriers to beetle movement were present (deep valleys, broad bodies of water and high-altitude ridges), potentially obscuring the power law relationship

motility habitat, which reduces travel time, with impact occurring at the boundaries. For MPB, this includes forest edges and boundaries of areas with low host density. Thinning is a control strategy prescribed to reduce the overall number of hosts and encounter rates for weakened hosts, in addition to increasing host vigour (Fettig, Gibson, Munson, & Negrón, 2014; Waring & Pitman, 1985). Inconsistency in the spatial pattern of thinning, however, could produce movement corridors with few hosts thereby resulting in accelerated MPB spread across a landscape. On the other hand, directly manipulating variation in host density may be a strategy for control of MPB. If

patches of high host density are small enough, they may act as ecological traps (Gilroy & Sutherland, 2007) for dispersing beetles. For example, in the related species southern pine beetle (*D. frontalis*), spot extinction risk increases dramatically as the number of hosts involved decreases (Friedenberg, Powell, & Ayres, 2007; Hedden & Billings, 1979).

Indirect control measures to reduce MPB population size (e.g. insecticides, semiochemicals and removal of infested hosts) could benefit by considering that MPB spread may be fastest through areas of low host density including along meadows and other clearings.

Consequently, control measures directed along boundaries of minimum travel time corridors are likely to have disproportionately large rewards. Using the power-law model and estimates of host tree density, travel time maps for MPB spread across a landscape can be calculated, helping to prioritize treatment application.

5 | CONCLUSION

The relationship between active aggregation to overcome the Allee effect and the patchy spread of populations has not been previously considered. The mechanisms evaluated here, differential dispersal reflecting landscape resistance to movement and active aggregation to overcome a strong Allee effect at low population densities, are reasonably general. Exponential representations of habitat influence on residence times are the most frequent model for landscape resistance to movement (e.g. Hanks & Hooten, 2013). Any Poisson process for encountering spot nucleation conditions will generate exponential failure probabilities for stopping in pixels. As discussed in Newman (2005), the combination of such exponential effects is a common way for power laws to arise in nature. We have shown that for MPB these exponential mechanisms do, in fact, combine to create power-law distributions of observable patchy spread.

There is a long history of considering the consequences of Allee effects on the passive dispersal and spread of organisms (see reviews by Liebhold & Tobin, 2008; Taylor & Hastings, 2005). Generally speaking, the Allee effect is expected to slow down invasions (Kot, Lewis, & den Driessche, 1996). The inertia of a strong Allee effect diminishes spread rates because small populations (below threshold) cannot establish away from the perimeter and “pull” the wave of invasion; source populations behind the perimeter of the wave of invasion must grow sufficiently to “push” out enough dispersers to overcome the Allee effect. Put more mathematically, the Allee effect truncates the passive dispersal kernel so that even fat-tailed (including power-law) kernels end up with finite moments, making the *effective* mean dispersal distance much smaller than the kernel's mean dispersal distance. Thus, with passive dispersal Allee effects slow or stop the spread of invasives. Invasions that would otherwise accelerate become constant speed invasions in the presence of the Allee effect (Wang, Kot, & Neubert, 2002); in heterogeneous environments, the Allee effect can stop invasions through “range pinning” (Keitt, Lewis, & Holt, 2001).

We have shown that active dispersal and spot formation due to the Allee effect result in power-law dispersal of propagules (spots) spreading from the perimeter of invaded areas. This is analogous to classic examples of species invasions *without* the Allee effect (Andow, Kareiva, Levin, & Okubo, 1990; Shigesada & Kawasaki, 1997; Skellam, 1951), and we therefore propose that the dispersed spots of impact “pull” the wave of invasion. As low-exponent power-law kernels may have only one moment, spread rates are limited only by the number of times the dispersal pattern is sampled (i.e. 75–83 times per kilometre of ever-expanding perimeter), leading to accelerating invasions (Clark, Lewis, & Horvath, 2001) in spite of an obvious Allee effect. These

mechanisms could have contributed to the recent rapid spread of MPB across western Canada (de la Giroday, Carroll, & Aukema, 2012).

ACKNOWLEDGEMENTS

The authors thank Tom Edwards and Ethan White for formative discussions and feedback, as well as three anonymous reviewers who offered many excellent suggestions. The USDA Forest Service Western Wildlands Environmental Threat Assessment Center provided support through a cooperative agreement with USU. This project was also supported in part by the Small Business Innovation Research (SBIR) programme of the USDA National Institute for Food and Agriculture (NIFA).

AUTHORS' CONTRIBUTIONS

B.B. and J.P. procured data used in this paper; N.F., B.B. and J.P. designed analyses; while M.G. and J.P. organized and implemented computational approaches used in the analyses; B.B. and N.F. provided ecological background on mountain pine beetle; and J.P. led the writing of the manuscript. All authors contributed critically to the drafts and gave final approval for publication.

DATA ACCESSIBILITY

Data used in this paper are archived in Utah State University's Digital Commons, http://digitalcommons.usu.edu/all_datasets/24/ (Powell, 2017; <https://doi.org/10.15142/T31C73>).

REFERENCES

- Allee, W. C. (1931). Co-operation among animals. *American Journal of Sociology*, 37, 386–398.
- Andow, D. A., Kareiva, P. M., Levin, S. A., & Okubo, A. (1990). Spread of invading organisms. *Landscape Ecology*, 4, 177–188.
- Berryman, A. A., Dennis, B., Raffa, K. F., & Stenseth, N. C. (1985). Evolution of optimal group attack, with particular reference to bark beetles (Coleoptera: Scolytidae). *Ecology*, 11, 898–903.
- Blackard, J. A., Finco, M. V., Helmer, E. H., Holden, G. R., Hoppus, M. L., Jacobs, D. M., ... Tycio, R. P. (2008). Mapping U.S. forest biomass using nationwide forest inventory data and moderate resolution information. *Remote Sensing of Environment*, 112, 1658–1677.
- Boone, C. K., Aukema, B. H., Bohlmann, J., Carroll, A. L., & Raffa, K. F. (2011). Efficacy of tree defense physiology varies with bark beetle population density: A basis for positive feedback in eruptive species. *Canadian Journal of Forest Research*, 41, 1174–1188.
- Boone, C. K., Keefover-Ring, K., Mapes, A. C., Adams, J., Bohlmann, A. S., & Raffa, K. F. (2013). Bacteria associated with a tree-killing insect reduce concentrations of plant defense compounds. *Journal of Chemical Ecology*, 39, 1003–1006.
- Carroll, A. L., Aukema, B. H., Raffa, K. F., Linton, D. A., Smith, G. D., & Lindgren, B. S. (2006). Mountain pine beetle outbreak development: The endemic-incipient epidemic transition. *Canadian Forest Service, Mountain Pine Beetle Initiative Project*, 1, 22.
- Chapman, T. B., Veblen, T. T., & Schoennagel, T. (2012). Spatiotemporal patterns of mountain pine beetle activity in the southern Rocky Mountains. *Ecology*, 93, 2175–2185.

- Choulakian, V., Lockhart, R. A., & Stephens, M. A. (1994). Cramér-von Mises statistics for discrete distributions. *The Canadian Journal of Statistics*, 22, 125–137.
- Clark, J. S., Lewis, M., & Horvath, L. (2001). Invasion by extremes: Population spread with variation in dispersal and reproduction. *The American Naturalist*, 157, 537–554.
- Crabb, B. A., Powell, J. A., & Bentz, B. J. (2012). Development and assessment of 30-m pine density maps for landscape-level modeling of mountain pine beetle dynamics. Res. Pap. RMRS-RP-96WWW (p. 43). U.S. Department of Agriculture, Forest Service, Rocky Mountain Research Station, Fort Collins, CO.
- de la Giroday, H. M. C., Carroll, A. L., & Aukema, B. H. (2012). Breach of the northern Rocky Mountain geoclimatic barrier: Initiation of range expansion by the mountain pine beetle. *Journal of Biogeography*, 39, 1112–1123.
- ESRI. (2008). *ArcGIS desktop: Release 9.3*. Redlands, CA: Environmental Systems Research Institute.
- Fettig, C. J., Gibson, K. E., Munson, A. S., & Negrón, J. F. (2014). Cultural practices for prevention and mitigation of mountain pine beetle infestations. *Forest Science*, 60, 450–463.
- Friedenberg, N. A., Powell, J. A., & Ayres, M. P. (2007). Synchrony's double edge: Transient dynamics and the Allee effect in stage structured populations. *Ecology Letters*, 10, 564–573.
- Garlick, M. J., Powell, J. A., Hooten, M. B., & McFarlane, L. R. (2011). Homogenization of large-scale movement models in ecology. *Bulletin of Mathematical Biology*, 73, 2088–2108.
- Gilroy, J. J., & Sutherland, W. J. (2007). Beyond ecological traps: Perceptual errors and undervalued resources. *Trends in Ecology and Evolution*, 22, 351–356.
- Goheen, D. & Hansen, E. (1993). Effects of pathogens and bark beetles on forests. In T. D. Schowalter & G. M. Filip (Eds.), *Beetle-pathogen interactions in conifer forests* (pp. 175–196). London, UK: Academic Press.
- Greene, C. M. (2003). Habitat selection reduces extinction of populations subject to Allee effects. *Theoretical Population Biology*, 64, 1–10.
- Halsey, R. (1998). *Aerial detection survey metadata for the Intermountain Region 4*. Ogden, UT: U.S. Department of Agriculture Forest Service, Forest Health Protection.
- Hanks, E. M., & Hooten, M. B. (2013). Circuit theory and model-based inference for landscape connectivity. *Journal of the American Statistical Association*, 108, 22–33.
- Hedden, R. L., & Billings, R. F. (1979). Southern pine beetle: Factors influencing the growth and decline of summer infestations in east Texas. *Forest Science*, 25, 547–556.
- Kane, J. M., & Kolb, T. E. (2010). Importance of resin ducts in reducing ponderosa pine mortality from bark beetle attack. *Oecologia*, 164, 601–609.
- Keitt, T. H., Lewis, M. A., & Holt, R. D. (2001). Allee effects, invasion pinning, and species borders. *The American Naturalist*, 157, 203–216.
- Kot, M., Lewis, M. A., & den Driessche, P. (1996). Dispersal data and the spread of invading organisms. *Ecology*, 77, 2027–2042.
- Lande, R. (1998). Demographic stochasticity and Allee effect on a scale with isotropic noise. *Oikos*, 83, 353–358.
- LEMMA. (2005). LEMMA: The GNNFire project [Homepage of the Landscape Ecology, Modeling, Mapping & Analysis research group of the USDA Forest Service Pacific Northwest Research Station and Oregon State University]. [Online]. Retrieved from <http://www.fsl.orst.edu/lemma/main.php?project=gnnfire&id=mapProducts> (accessed October 24, 2010).
- Liebold, A. M., & Tobin, P. C. (2008). Population ecology of insect invasions and their management. *Annual Review of Entomology*, 53, 387–408.
- Logan, J. A., White, P., Bentz, B. J., & Powell, J. A. (1998). Model analysis of spatial patterns in mountain pine beetle outbreaks. *Theoretical Population Biology*, 53, 236–255.
- Meddens, A. J. H., Hicke, J. A., & Ferguson, C. A. (2012). Spatiotemporal patterns of observed bark beetle-caused tree mortality in British Columbia and the western United States. *Ecological Applications*, 22, 1876–1891.
- Mitchell, R. G., & Preisler, H. K. (1991). Analysis of spatial patterns of lodgepole pine attacked by outbreak populations of the mountain pine beetle. *Forest Science*, 37, 1390–1408.
- Morozov, A., Petrovskii, S., & Li, B. L. (2006). Spatiotemporal complexity of patchy invasion in a predator-prey system with the Allee effect. *Journal of Theoretical Biology*, 238, 18–35.
- Newman, M. E. (2005). Power laws, Pareto distributions and Zipf's law. *Contemporary Physics*, 46, 323–351.
- Okubo, A., & Levin, S. A. (2001). *Diffusion and ecological problems: Modern perspectives* (Vol. 14). New York, NY: Springer-Verlag.
- Patlak, C. S. (1953). Random walk with persistence and external bias. *The Bulletin of Mathematical Biophysics*, 15, 311–338.
- Petrovskii, S. V., Morozov, A. Y., & Venturino, E. (2002). Allee effect makes possible patchy invasion in a predator-prey system. *Ecology Letters*, 5, 345–352.
- Pfeifer, E. M., Hicke, J. A., & Meddens, A. J. H. (2011). Observations and modeling of aboveground tree carbon stocks and fluxes following a bark beetle outbreak in the western United States. *Global Change Biology*, 17, 339–350.
- Pierce, K. B., Ohmann, J. L., Wimberly, M. C., Gregory, M. J., & Fried, J. S. (2009). Mapping wildland fuels and forest structure for land management: A comparison of nearest neighbor imputation and other methods. *Canadian Journal of Forest Research*, 39, 1901–1916.
- Powell, J. A. (2017). MPB spot infestation data. DigitalCommons@USU. Dataset, <https://doi.org/10.15142/T31C73>
- Powell, J. A., & Bentz, B. J. (2009). Connecting phenological predictions with population growth rates for mountain pine beetle, an outbreak insect. *Landscape Ecology*, 24, 657–672.
- Powell, J. A., & Bentz, B. J. (2014). Phenology and density-dependent dispersal predict patterns of mountain pine beetle (*Dendroctonus ponderosae*) impact. *Ecological Modelling*, 273, 173–185.
- Raffa, K. F., Aukema, B. H., Erbilgin, N., Klepzig, K. D., & Wallin, K. F. (2005). Chapter Four Interactions among conifer terpenoids and bark beetles across multiple levels of scale: An attempt to understand links between population patterns and physiological processes. *Recent Advances in Phytochemistry*, 39, 79–118.
- Raffa, K. F., Aukema, B. H., Bentz, B. J., Carroll, A. L., Hicke, J. A., Turner, M. G., & Romme, W. H. (2008). Cross-scale drivers of natural disturbances prone to anthropogenic amplification: Dynamics of biome-wide bark beetle eruptions. *BioScience*, 58, 501–518.
- Raffa, K. F., Powell, E. N., & Townsend, P. A. (2012). Temperature-driven range expansion of an irruptive insect heightened by weakly coevolved plant defense. *PNAS*, 110, 2193–2198.
- Safranyik, L., & Carroll, A. (2006). The biology and epidemiology of the mountain pine beetle in lodgepole pine forests. In L. Safranyik & B. Wilson (Eds.), *The mountain pine beetle: A synthesis of biology, management, and impacts on lodgepole pine* (pp. 3–66). Victoria, BC: Natural Resources Canada, Canadian Forest Service.
- Safranyik, L., Linton, D. A., Silversides, R., & McMullen, L. H. (1992). Dispersal of released mountain pine beetles under the canopy of a mature lodgepole pine stand. *Journal of Applied Entomology*, 113, 441–450.
- Sharov, A. A., & Liebhold, A. M. (1998). Model of slowing the spread of gypsy moth (Lepidoptera: Lymantriidae) with a barrier zone. *Ecological Applications*, 8, 1170–1179.
- Shigesada, N., & Kawasaki, K. (1997). *Biological invasions: Theory and practice*. Oxford, UK: Oxford University Press.
- Skellam, J. G. (1951). Random dispersal in theoretical populations. *Biometrika*, 38, 196–218.
- Stephens, P. A., Sutherland, W. J., & Freckleton, R. P. (1999). What is the Allee effect? *Oikos*, 87, 185–190.
- Taylor, C. M., & Hastings, A. (2005). Allee effects in biological invasions. *Ecology Letters*, 8, 895–908.
- Taylor, C. M., Davis, H. G., Civille, J. C., Grevstad, F. S., & Hastings, A. (2004). Consequences of an Allee effect in the invasion of a Pacific estuary by *Spartina alterniflora*. *Ecology*, 85, 3254–3266.

- Turchin, P. (1989). Population consequences of aggregative movement. *The Journal of Animal Ecology*, 58, 75–100.
- Turchin, P. (1998). *Quantitative analysis of movement*. Sunderland, MA: Sinauer Associates, Inc.
- Wang, M. H., & Kot, M. (2001). Speeds of invasion in a model with strong or weak Allee effects. *Mathematical Biosciences*, 171, 83–97.
- Wang, M. H., Kot, M., & Neubert, M. G. (2002). Integrodifference equations, Allee effects, and invasions. *Journal of Mathematical Biology*, 44, 150–168.
- Wang, J., Shi, J., & Wei, J. (2011). Dynamics and pattern formation in a diffusive predator-prey system with strong Allee effect in prey. *Journal of Differential Equations*, 251, 1276–1304.
- Waring, R. H., & Pitman, G. B. (1985). Modifying lodgepole pine stands to change susceptibility to mountain pine beetle attack. *Ecology*, 66, 889–897.
- Wertheim, B., van Baalen, E. J. A., Dicke, M., & Vet, L. E. (2005). Pheromone-mediated aggregation in nonsocial arthropods: An evolutionary ecological perspective. *Annual Review of Entomology*, 50, 321–346.
- Zhao, H. (2004). A fast sweeping method for eikonal equations. *Mathematics of Computation*, 74, 603–627.

How to cite this article: Powell JA, Garlick MJ, Bentz BJ, Friedenber N. Differential dispersal and the Allee effect create power-law behaviour: Distribution of spot infestations during mountain pine beetle outbreaks. *J Anim Ecol*. 2017;00:1–14. <https://doi.org/10.1111/1365-2656.12700>